J Mater Sci (2009) 44:1952–1958
DOI 10.1007/s10853-009-3287-0

Effects of processing parameters on the refinement of primary Si in A390 alloys with a new Al–Si–P master alloy

Min Zuo · Xiangfa Liu · Qianqian Sun

Received: 19 September 2008 / Accepted: 20 January 2009 / Published online: 26 February 2009

Abstract In this study, a new Al–17Si–2.5P master alloy has been successfully prepared to refine primary Si in hypereutectic A390 alloys. By means of electron probe microanalyzer (EPMA), a large number of AlP particles can be found in the Al–17Si–2.5P master alloy. An orthogonal $L_9(3^3)$ test was designed to investigate the integrated effects of refining factors including phosphorus addition level, melting temperature and holding time, and subsequently to optimize the processing parameters. It is found that under the optimized conditions, i.e., phosphorus addition of 375 ppm, melting temperature of 800 °C, and holding time of 30 min, the average sizes of primary Si can be most remarkably decreased from 116 μm to 14 μm with sphere-like morphology. Meanwhile, the Brinell hardness and tensile strength can be significantly increased by 14.1 and 27.8%, respectively. In addition, thermal analysis is also performed with differential scanning calorimeter (DSC) to analyze the solidification process of Al–18Si alloys.

M. Zuo · X. Liu (✉)
Key Laboratory of Liquid Structure and Heredity of Materials, Ministry of Education, Shandong University, 73 Jingshi Road, Jinan 250061, People's Republic of China
e-mail: xfliu@sdu.edu.cn

M. Zuo
e-mail: zuomin1101@yahoo.cn

X. Liu
Shandong Binzhou Bohai Piston Co., Ltd, Binzhou, Shandong 256602, People's Republic of China

Q. Sun
Shandong Shanda Al & Mg Melt Tech. Co., Ltd, Jinan, Shandong 250061, People's Republic of China

Introduction

Considerable efforts have been devoted to the development of hypereutectic Al–Si alloys, due to their excellent wear and corrosion resistance, lower density, higher thermal stability, and outstanding mechanical properties [1–3]. However, the primary Si particles in hypereutectic Al–Si alloys exhibit rather irregular morphologies, such as coarse platelet and polygon, which cause the serious disseverance to the matrix [4, 5]. In the past decades, various techniques have been developed to resolve this problem, and the excellent refinement efficiency of primary Si can be obtained through addition of some modifiers, such as P [6–14], As [15], rare earth (RE) [5, 16–18], etc. Among these modifiers, P is one of the most effective refiner of primary Si particles and can be added into the melt in many forms, such as red phosphorus, phosphate salt, Cu–P [6–9], Al–Cu–P, and Al–Fe–P [13, 14]. However, red phosphorus and phosphate salt are less utilized mainly due to the pollution to the environment, unstable modification efficiency, and lower P recovery. According to the reference [9], Cu–P master alloy is relatively more stable to be used as a modifier compared to Al–Cu–P master alloy, but higher modification temperature is necessary. Meanwhile, the use of Al–Fe–P master alloy would cause the contamination of Fe in composition. Therefore, the AlP-containing master alloy without other impurity elements is thought to be an ideal P addition for the modification and refinement of primary Si in Al–Si alloys.

Many researches into the refinement of primary Si have usually focused on a single or two factors, such as modifier, temperature, holding time, etc. Robles Hernandez and Sokolowski [7] reported that two parameters had major influence on Si modification: one was the temperature at which the melt treatment was operated and the other was

the chemical modifiers. While Maeng et al. [9] proposed that the most important factors to influence the refinement of primary Si particles were melt temperature and holding time. However, the integrated and systematic effects of these factors have been given little consideration [18].

In this study, a new Al–17Si–2.5P master alloy was applied, and the processing parameters of refining treatment, i.e., phosphorus addition level, melting temperature, and holding time, were optimized through an orthogonal $L_9(3^3)$ test. Meanwhile, the Brinell hardness and tensile strength of samples were also measured.

Experimental procedures

The base alloys used in this study were hypereutectic A390 alloys (17.0Si, 4.5Cu, 0.5Mg, and balance Al, all in wt%), which were prepared by commercial purity Al (99.85%), Si (99.5%), and other commercial purity elements using medium frequency induction furnace. The Al–17Si–2.5P master alloy was developed by collaboration with Shandong Shanda Al&Mg Melt Technology Co. Ltd.

The refining treatments of A390 alloys designed in the orthogonal test were carried out with the same procedures as follows. The base alloy was remelted in a graphite crucible using an electrical resistance furnace and kept at the temperature for 30 min. Then the melt was degassed with C_2Cl_6 for 15 min, and the refining treatment was carried out with the addition of Al–17Si–2.5P master alloy. After different holding times, the melt was poured into a permanent mold ($70 \times 35 \times 20$ mm^3) preheated to 150 °C. The pouring mold used in the refining treatments is illustrated in Fig. 1.

The detailed microstructure analysis was carried out on the A390 samples to investigate the influence of processing parameters on refinement and to study the heterogeneous nucleating role of AlP particles on primary Si. Metallographic specimens of A390 alloys were all cut from the same position of the casting samples, mechanically ground, and then polished through standard routines. Statistical analysis was conducted to determine the average size of primary Si. What should be noted is that, it is necessary to fast prepare the specimens of the Al–17Si–2.5P master alloy to avoid oxidation and hydrolysis of AlP. The microstructure analysis was carried out with High Scope Video Microscope (HSVM) and JXA-8840 Electron Probe Microanalyzer (EPMA). The Brinell hardness was measured following the standard of HB10-1000, which means a 9807 N load and 10-mm diameter indenter with a loading time of 15 s. Meanwhile, the tensile strength at room temperature was studied using a universal testing machine (CMT700). Thermal analysis was performed with differential scanning calorimeter (DSC) to analyze the solidification process of Al–18Si alloys with addition of the Al–17Si–2.5P master alloy.

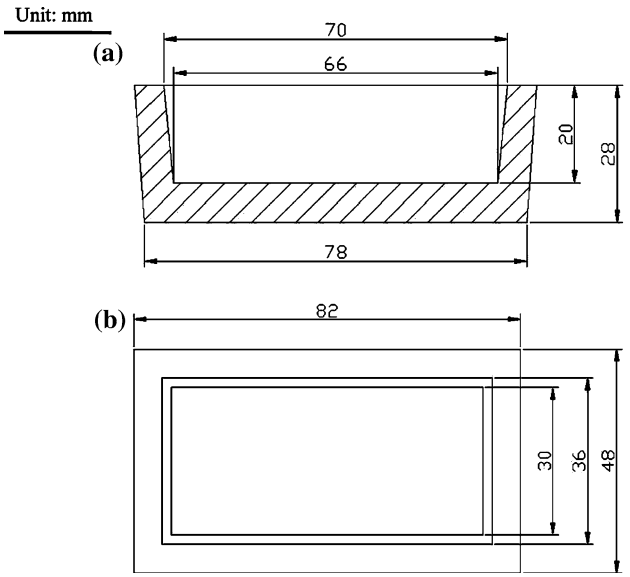

Fig. 1 Pattern dimensions of the pouring mold used in grain refining tests: **a** sectional view and **b** vertical view

Results and discussion

Microstructure characterizations of Al–17Si–2.5P master alloy

Figure 2 shows the EPMA analysis of Al–17Si–2.5P master alloy. It can be seen that the Al–17Si–2.5P master alloy is composed of three phases: α-Al, Si phase (primary Si and eutectic Si), and AlP particles. It is worth noting that there are a large number of AlP particles contained in the master alloy. Meanwhile, it can be found that the Si phase presents uniform distribution alongside of AlP particles due to their similar crystal structure and lattice parameters. In addition, the AlP particles contained in the Al–17Si–2.5P master alloy exhibit two morphologies: plate-like and sphere-like, which may be attributed to the aggregation of AlP particles during solidification process.

Effects of processing parameters on the refinement of primary Si

Orthogonal test design is an efficient and scientific method which investigates the relative importance of various factors and identifies the best levels for different factors [19]. Since various processing parameters influence the refinement effect of modifiers on primary Si, the optimization of the experimental conditions is the critical step in the refining treatment of primary Si. In fact, phosphorus

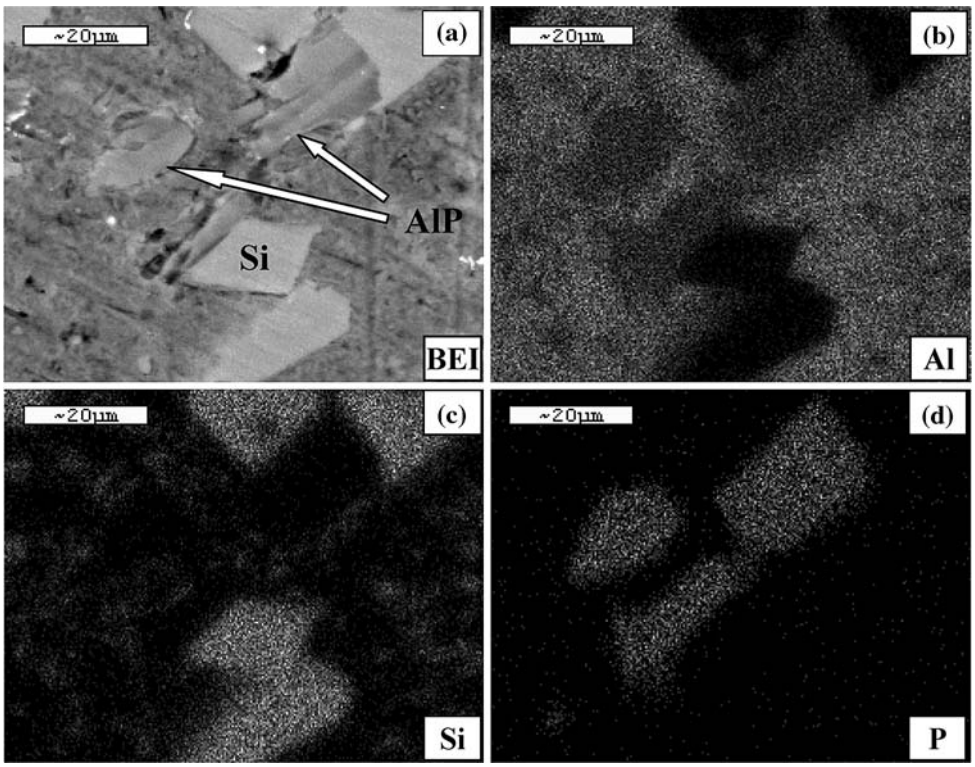

Fig. 2 EPMA analysis of Al–17Si–2.5P master alloy: **a** BEI and **b–d** the X-ray images for element: Al, Si, and P, respectively

addition level, melting temperature, and holding time are generally considered to be the most important factors. Each at three levels, the three factors are presented in Table 1.

According to the experimental design theory, an orthogonal array $L_9(3^3)$ is selected to arrange the test programs. The meanings of all numbers in $L_9(3^3)$ are illustrated in Fig. 3. All the nine experiments arrayed in the orthogonal test were carried out with their respective combination of phosphorus addition, melting temperature, and holding time. The evaluation index in the present study was the average size of primary Si particles. K is the sum of the average size of primary Si at the same level of each factor. For example, K_1^A means the sum of the mean value of primary Si for factor A at level 1 and is obtained by the formula as follows: $22.6 + 23.1 + 18.8 = 64.5$. The k is the mean value corresponding to K. By comparing with values of different k, the optimal level of factors can be confirmed. The R value for each factor is produced by subtracting the minimum value from the corresponding maximum value among the k_1, k_2, and k_3 rows. For example the R value for factor A is: $21.5 - 17.0 = 4.5$. The R value reflects the effects of factors on the result. The higher the R value is, the greater the influence of the factor on evaluation index will be [19–21].

Table 1 Factors and levels for the orthogonal test

Levels	Factors		
	(A) P addition level (ppm)	(B) Melting temperature (°C)	(C) Holding time (min)
1	125	750	30
2	250	800	60
3	375	850	90

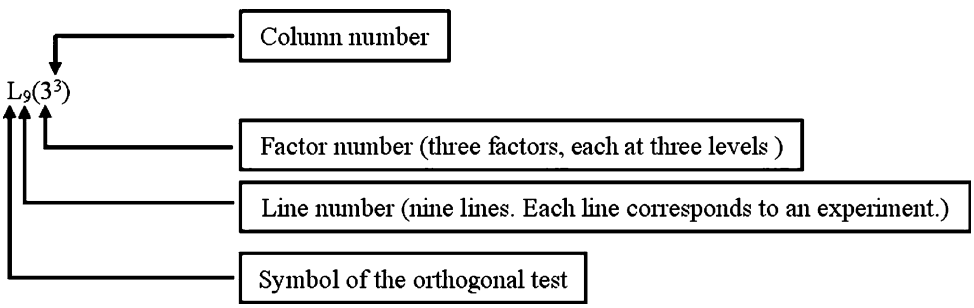

Fig. 3 The schematic diagram for meanings of numbers in $L_9(3^3)$ orthogonal test

Table 2 Experimental arrangement and test results

Test No.	Factors			Test results
	A (ppm)	*B* (°C)	*C* (min)	Mean sizes of primary Si (μm)
1	125	750	30	22.6
2	125	800	60	23.1
3	125	850	90	18.8
4	250	750	60	20.6
5	250	800	90	16.9
6	250	850	30	16.5
7	375	750	90	19.5
8	375	800	30	14.0
9	375	850	60	17.4
K_1	64.5	62.7	53.1	–
K_2	54.0	54.0	61.1	
K_3	50.9	52.7	55.2	
k_1	21.5	20.9	17.7	
k_2	18.0	18.0	20.4	
k_3	17.0	17.6	18.4	
R	4.5	3.3	2.7	–

$K_i^F = \sum$ the average size of primary Si at the same level of each factor

$k_i^F = K_i^F/3$

$R^F = \max\{k_i^F\} - \min\{k_i^F\}$ (F stands for factors A, B and C, $i = 1, 2, 3$)

The results of the orthogonal test are listed in Table 2. In view of orthogonal test analysis, it can be found that the influencing extent of the three factors decreases in the order: $A > B > C$ according to the R value. The addition level of phosphorus is found to be the most important factor to the refinement of primary Si. The average size of primary Si decreased significantly from 21.5 μm to 17.0 μm as the concentration of phosphorus (factor *A*) increased from 125 ppm to 375 ppm, as shown in Table 2. In comparison with that, the melting temperature (factor *B*) has a relatively minor effect on the refinement efficiency of primary Si. With the melting temperature increasing from 750 to 850 °C, the average size of primary Si changes from 20.9 μm to 17.6 μm. The holding time (factor *C*) has the minimum influence compared with other two factors.

The variations of average size of primary Si with the three factors are shown in Fig. 4. Based on the relationship between the factors and the mean size of primary Si shown in Fig. 4, the optimal processing parameters for the refinement of primary Si in hypereutectic A390 alloys refined by Al–17Si–2.5P master alloy are phosphorus addition of 375 ppm, melting temperature of 850 °C, and holding time of 30 min (*A*3–*B*3–*C*1). An experimental confirmation was carried out and the result is shown in Fig. 5. The primary Si in untreated A390 alloys presents irregular morphologies such as coarse platelet and branch-like, which will crack Al matrix easily. It can be seen that in Fig. 5b and c, the A390 alloys have shown fast grain refinement response to the addition of Al–17Si–2.5P master alloys, with the average size of primary Si significant decreasing significantly from 116 μm to about 20 μm by statistical analysis. Meanwhile, the morphologies of primary Si change into sphericity from other irregular morphologies. Furthermore, the average size of primary Si refined under the predicted optimal conditions (*A*3–*B*3–*C*1) in Fig. 5c is about 21.8 μm, larger than that of test No. 8 (*A*3–*B*2–*C*1) which shows the most excellent refinement effect compared with all the other experiments in Table 2. These results indicate the optimal conditions for the refinement of primary Si in A390 alloys: phosphorus addition of 375 ppm, melting temperature of 800 °C, and holding for 30 min (*A*3–*B*2–*C*1).

Mechanical properties of A390 alloys refined by Al–17Si–2.5P master alloy

The Brinell hardness (HB) and tensile strength at room temperature of the unrefined and refined A390 alloys are listed in Table 3. In comparison with the unrefined alloys, the Brinell hardness value of refined A390 samples under the optimized conditions from the orthogonal test listed

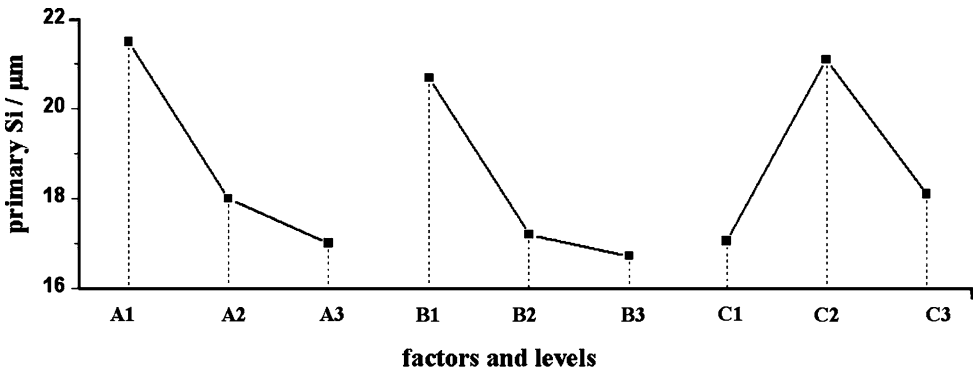

Fig. 4 The relationship between factors and results in the orthogonal test

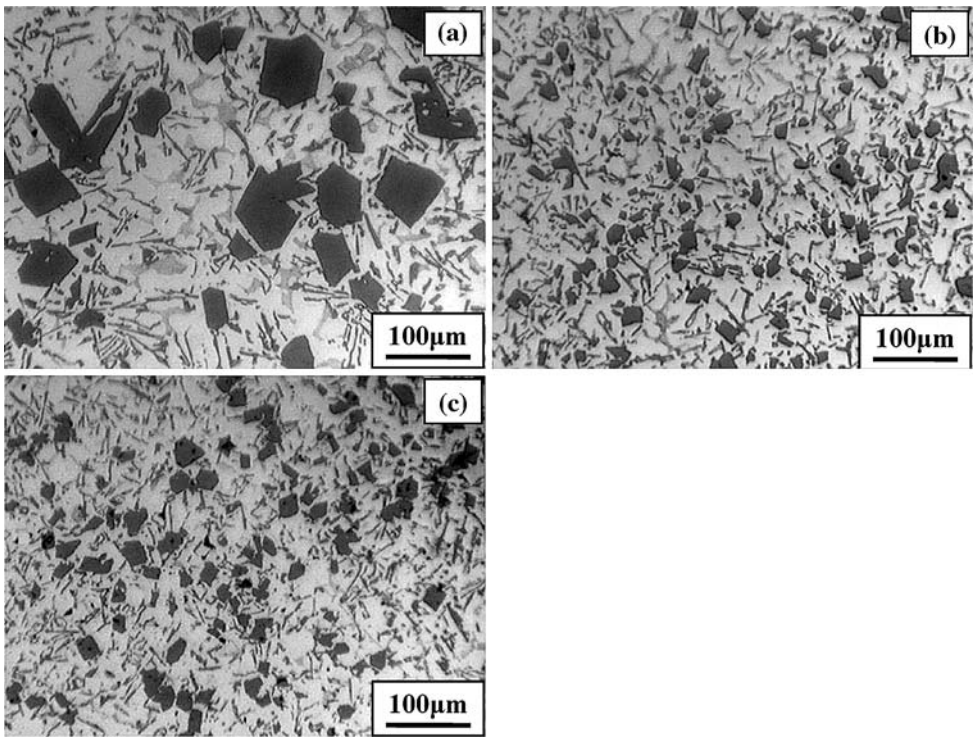

Fig. 5 Microstructures of A390 alloys: **a** without Al–Si–P addition, **b** A390 + 1.5% Al–17Si–2.5P (Test No.8: *A*3–*B*2–*C*1), **c** A390 + 1.5% Al–17Si–2.5P (treated with the predicted optimal processing parameters: *A*3–*B*3–*C*1)

Table 3 Mechanical properties of the investigated A390 alloys

Alloy	Treating method	HB	$\sigma_{b,20\ ^\circ C}$/MPa
A390 (as-cast)	Unrefined sample	113	150.2
	Refined by Al–17Si–2.5P master alloy with parameters of *A*3–*B*2–*C*1	129	191.9

above is much higher and is increased remarkably by about 14.1%. Meanwhile, the tensile strength of A390 alloys is also significantly improved, which is increased by about 27.8%. Previous studies have illustrated that the mechanical properties of Al–Si alloys are closely interrelated to their microstructural characters [5, 9, 10]. It is thought that the significant improvement of the mechanical properties is attributed to the refinement of primary Si caused by the heterogeneous nuclei of AlP particles contained in Al–17Si–2.5P master alloy.

Refinement mechanism of Al–17Si–2.5P master alloy

It is well established that AlP is zinc blende structure with lattice parameter $a = 0.545$ nm. As shown in Fig. 6, it can be seen that the Al atoms form a face-centered cubic array, and the P atoms fill on half of the tetrahedral holes with each P atom surrounded by four proximate Al atoms [22–24].

According to the literatures [10, 25–27], Si can nucleate heterogeneously on a substrate of AlP with a cube–cube

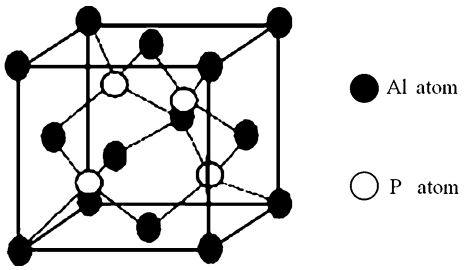

Fig. 6 Crystal structure of AlP

orientation relationship and solidify to form a faceted Si particle due to the very similar lattice parameters with AlP. Furthermore, Ma [28] reported that both adsorption and wetting should be treated as a mechanism for nucleation on potent/wettable substrates. However, Ma also pointed out that, when considering nucleation in atomic dimensions, adsorption is a more functional mechanism than wetting. Figure 7 shows the EPMA analysis for the A390 alloys with addition of Al–17Si–2.5P master alloy which proves the existence of AlP particles in conjunction with primary Si.

As illustrated in Fig. 5, the refinement effect is deteriorated with the melting temperature rising from 800 to 850 °C. The result can be explained as follows. It is well known that when adding P modifiers into the melt, a large quantity of AlP particles cannot uniformly distribute in the melt due to the lower solubility of phosphorus and the density difference. The undissolved AlP particles would become the dregs and float to the surface and cannot act as

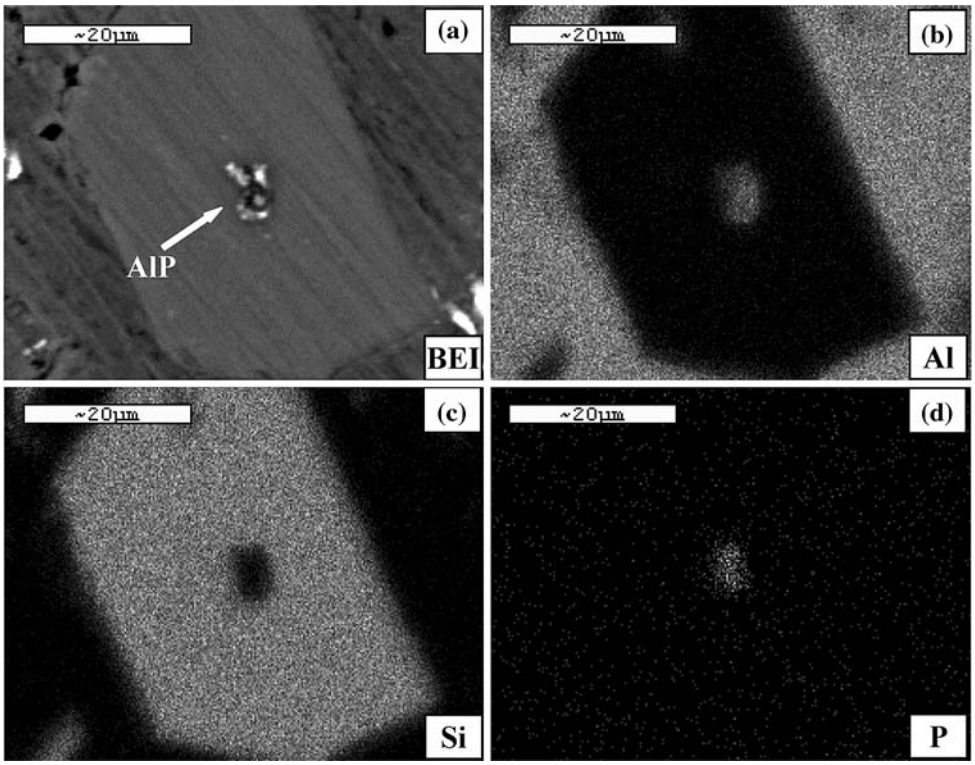

Fig. 7 EPMA analysis of A390 alloys with addition of Al–17Si–2.5P master alloys: **a** BEI and **b–d** the X-ray images for element: Al, Si, and P, respectively

the nucleation sites of primary Si during solidification process. With the temperature decreasing in solidification process, the AlP particles which are homogeneously dissolved in the melt mentioned above would precipitate, and this part of AlP particles is usable for the modifier to display excellent refining performance [22, 24, 29]. According to the theory proposed by Beer and Lescuyer et al. [25, 30], the solubility of AlP can be calculated as follows: $\log(x_P) = 0.684 - \frac{4986}{T}$, where x_P is the molar fraction of soluble phosphorus and T is the Kelvin temperature. From the equation, it can be found that the solubility of AlP increases with the elevation of temperature, which agrees well with the Arrhenius equation. Combined with the verification experiment to the orthogonal test, the solubility of AlP at 850 °C is relatively higher than that of AlP particles at 800 °C.

In order to analyze the solidification processes of A390 alloys with different addition of P modifiers, thermal analysis was performed with DSC. The Al–18Si alloys prepared by high-purity Al and high-purity crystalline Si were used as the base alloy, and the results are shown in Fig. 8 (Additionally, it is worth noting the DSC curves for each sample in Fig. 8 have been offset for presentation clarity.). It can be seen that before Al–17Si–2.5P master alloy addition, there are two exothermic peaks at about 652.0 °C and 567.8 °C shown by curve (a), which correspond to the precipitation of primary Si and the eutectic reaction, respectively. From the curves (b) and (c), it can be

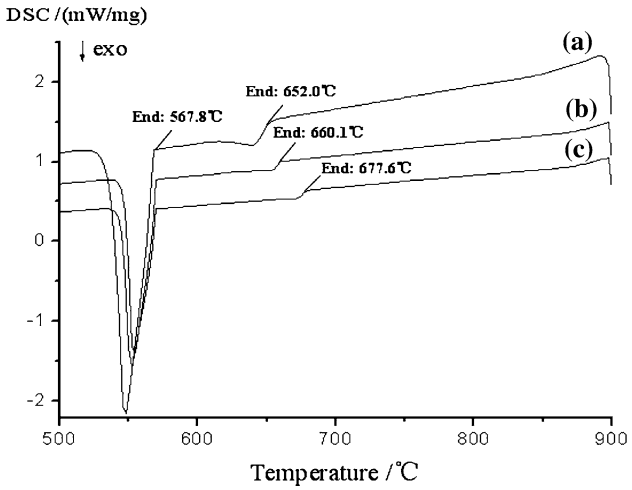

Fig. 8 DSC results for Al–18Si alloys: **a** without Al–Si–P addition, **b** Al–18Si + 1.5% Al–17Si–2.5P (Test No.8: *A*3–*B*2–*C*1), **c** Al–18Si + 1.5% Al–17Si–2.5P (treated with the predicted optimal processing parameters: *A*3–*B*3–*C*1)

observed that the peak corresponding to the precipitation of primary Si is shifted to higher temperature after the addition of AlP particles. Meanwhile, with the addition level of P increasing to 375 ppm, the beginning of the exothermic peak associating with precipitation of primary Si is shifted to 677.6 °C, about 17.5 °C higher than that of 250 ppm P addition. According to the literature [7], the time for coarsening of primary Si in solidification process depends

directly on the time from the beginning of growth. It is considered that the Si growth time in the treated A390 alloys with *A*3–*B*3–*C*1 is relatively longer than that of *A*3–*B*2–*C*1, which causes the coarsening of primary Si as shown in Fig. 5c.

Conclusions

(1) A new Al–17Si–2.5P master alloy with a large number of pre-formed AlP particles has been successfully prepared to refine primary Si in hypereutectic A390 alloys.

(2) By means of orthogonal test, it is found that the refinement effect on primary Si is influenced by phosphorus addition level, melting temperature, and holding time, and the optimized conditions for the refinement of primary Si in A390 alloys are phosphorus addition of 375 ppm, melting temperature of 800 °C, and holding time of 30 min.

(3) Under the optimized conditions, the average size of primary Si can be remarkably decreased from 116 to about 14 μm, with sphere-like morphology and homogeneous distribution. The Brinell hardness and tensile strength can also be increased significantly by 14.1 and 27.8%, respectively.

Acknowledgements This work was supported by a grant from National Science Fund for Distinguished Young Scholars of China (No. 50625101), Key Project of Science and Technology Research of Ministry of Education of China (No. 106103), and "Taishan Scholar" Construction Project for financial support of Shandong Province in China.

References

1. Li J, Elmadagli M, Gertsman VY, Lo J, Alpas AT (2006) Mater Sci Eng A 421(1–2):317
2. Haque MM, Sharif A (2001) J Mater Process Technol 118(1–3):69
3. Srivastava VC, Mandal RK, Ojha SN (2004) Mater Sci Eng A 383(1):14
4. Kang HS, Yoon WY, Kim KH, Kim MH, Yoon YP (2005) Mater Sci Eng A 404(1–2):117
5. Jiang QC, Xu CL, Lu M, Wang HY (2005) Mater Lett 59(6):624
6. Zhang HH, Duan HL, Shao GJ, Xu LP (2008) Rare Met 27(1):59
7. Robles Hernandez FC, Sokolowski JH (2006) J Alloys Compd 426(1–2):205
8. Robles Hernandez FC, Sokolowski JH (2005) J Miner Met Mater Soc 57(11):48
9. Maeng DY, Lee JH, Won CW, Cho SS, Chun BS (2000) J Mater Process Technol 105(1–2):196
10. Liu XF, Qiao JG, Liu YX, Li ST, Bian XF (2004) Acta Metall Sin 40(5):471
11. Qiao JG, Liu XF, Liu XJ, Bian XF (2005) Mater Lett 59(14–15):1790
12. Liu XF, Wu YY, Bian XF (2005) J Alloys Compd 391(1–2):90
13. Kyffin WJ, Rainforth WM, Jones H (2001) J Mater Sci 36(11):2667. doi:10.1023/A:1017904627733
14. Faraji M, Todd I, Jones H (2005) J Mater Sci 40(24):6363. doi:10.1007/s10853-005-3103-4
15. Yilmaz F, Atasoy OA, Elliott R (1992) J Cryst Growth 118(3–4):377
16. Yi HK, Zhang D (2003) Mater Lett 57(16–17):2523
17. Chang JY, Kim GH, Moon IG, Choi CS (1998) Scr Mater 39(3):307
18. Wang ZH, Mao XM, Zhang JL, Ou Yang ZY (2005) Spec Cast Nonferrous Alloys 25(4):241
19. Alam HG, Moghaddam AZ, Omidkhah MR (2009) Fuel Process Technol 90(1):1
20. Liu CZ, Ren LQ, Tong J, Green SM, Arnell RD (2002) Wear 253(7–8):878
21. Peng JY, Dong FQ, Xu QW, Xu YW, Qi Y, Han X, Xu LN, Fan GR, Liu KX (2006) J Chromatogr A 1135(2):151
22. Yu LN, Liu XF, Ding HM, Bian XF (2007) J Alloys Compd 429(1–2):119
23. Li C, Liu XF, Wu YY (2008) J Alloys Compd 465(1–2):145
24. Yu LN, Liu XF, Ding HM, Bian XF (2007) J Alloys Compd 432(1–2):156
25. Lescuyer H, Allibert M, Laslaz G (1998) J Alloys Compd 279(2):237
26. Ho CR, Cantor B (1995) Acta Metall Mater 43(8):3231
27. Cantor B (1997) Mater Sci Eng A 226–228:151
28. Ma Q (2007) Acta Mater 55(3):943
29. Wu YY, Liu XF, Bian XF (2006) Mater Sci Eng A 427(1–2):69
30. Beer SZ (1969) J Electrochem Soc 116(2):263